PROCEEDINGS B

royalsocietypublishing.org/journal/rspb

Research

Cite this article: Welte L, Kelly LA, Kessler SE, Lieberman DE, D'Andrea SE, Lichtwark GA, Rainbow MJ. 2021 The extensibility of the plantar fascia influences the windlass mechanism during human running. *Proc. R. Soc. B* **288**: 20202095. https://doi.org/10.1098/rspb.2020.2095

Received: 2 September 2020
Accepted: 11 December 2020

Subject Category:
Morphology and biomechanics

Subject Areas:
biomechanics, physiology

Keywords:
foot arch biomechanics, plantar fascia, windlass mechanism, arch-spring, biplanar videoradiography, running

Author for correspondence:
Lauren Welte
e-mail: l.welte@queensu.ca

Electronic supplementary material is available online at https://doi.org/10.6084/m9.figshare.c.5251457.

THE ROYAL SOCIETY PUBLISHING

The extensibility of the plantar fascia influences the windlass mechanism during human running

Lauren Welte[1], Luke A. Kelly[2], Sarah E. Kessler[2,3], Daniel E. Lieberman[3], Susan E. D'Andrea[4], Glen A. Lichtwark[2] and Michael J. Rainbow[1]

[1]Department of Mechanical and Materials Engineering, Queen's University, Kingston, Ontario, Canada
[2]School of Human Movement and Nutrition Sciences, The University of Queensland, Brisbane, Queensland, Australia
[3]Department of Human Evolutionary Biology, Harvard University, Cambridge, MA, USA
[4]Department of Kinesiology, University of Rhode Island, Kingston, RI, USA

LW, 0000-0003-2218-3007; LAK, 0000-0002-9736-0517; DEL, 0000-0002-6194-9127

The arch of the human foot is unique among hominins as it is compliant at ground contact but sufficiently stiff to enable push-off. These behaviours are partly facilitated by the ligamentous plantar fascia whose role is central to two mechanisms. The ideal windlass mechanism assumes that the plantar fascia has a nearly constant length to directly couple toe dorsiflexion with a change in arch shape. However, the plantar fascia also stretches and then shortens throughout gait as the arch-spring stores and releases elastic energy. We aimed to understand how the extensible plantar fascia could behave as an ideal windlass when it has been shown to strain throughout gait, potentially compromising the one-to-one coupling between toe arc length and arch length. We measured foot bone motion and plantar fascia elongation using high-speed X-ray during running. We discovered that toe plantarflexion delays plantar fascia stretching at foot strike, which probably modifies the distribution of the load through other arch tissues. Through a pure windlass effect in propulsion, a quasi-isometric plantar fascia's shortening is delayed to later in stance. The plantar fascia then shortens concurrently to the windlass mechanism, likely enhancing arch recoil at push-off.

1. Introduction

Three key modifications in the foot thought to have been selected for bipedal walking and endurance running in hominins are the adducted great toe, the medial longitudinal arch and a relatively robust plantar fascia [1,2]. These derived features manage the load during weight acceptance and help the foot function as a stable lever during the push-off phase of walking and running. Two mechanisms that explain these passive characteristics of the foot are the arch-spring and windlass mechanisms [3,4]. The plantar fascia is fundamental to both mechanisms, as it spans the arch of the foot, connecting the calcaneus to the five proximal phalanges by wrapping around the metatarsal–phalangeal joints (MTPJs) [5]. As originally described, the arch-spring and windlass mechanisms require different plantar fascia behaviour.

The arch-spring, proposed by Ker *et al*. [3], conceptualizes the medial longitudinal arch as a dynamic truss with arch-spanning ligaments that serve as energy-saving springs. In their foundational study, the arch-supporting structures of a cadaver foot were sequentially cut, and the foot was subjected to compressive loads that simulated running forces. The authors projected that the arch stored and returned sufficient energy to make metabolic savings during running, which was confirmed in an *in vivo* study [6]. Furthermore, several studies have shown that the plantar fascia strains during stance [7–13], and that the arch of the foot stores less elastic energy without a plantar fascia [3], indicating that the plantar fascia contributes to the energy-saving arch-spring mechanism.

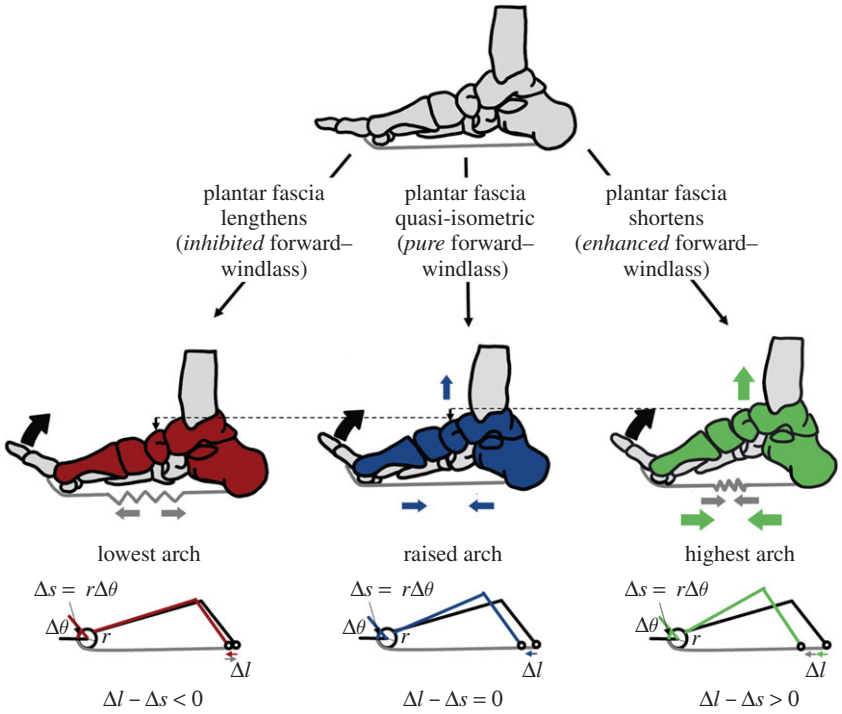

Figure 1. Theoretical framework. The forward-windlass mechanism's ability to shorten and raise the arch can be theoretically influenced if the plantar fascia simultaneously lengthens, shortens or is quasi-isometric. The pure forward-windlass mechanism occurs if there is a 1 : 1 ratio of arch deformation (Δl) to arc length change from MTPJ dorsiflexion ($\Delta s = r\Delta\theta$). If the plantar fascia shortens concurrently to the forward-windlass mechanism, it could enhance arch rising. If the plantar fascia lengthens simultaneously to the forward-windlass mechanism, the arch rising effect could be limited. (Online version in colour.)

In 1954, Hicks [4] described the plantar fascia's influence on the arch as a windlass mechanism. According to his description, dorsiflexion of the MTPJs pulls on the stiff plantar fascia, whose tissue encapsulates small sesamoid bones inferior to the metatarsal heads. The sesamoid bones and the firmly attached plantar fascia slide around the metatarsal head, pulling the calcaneus towards the phalanges, shortening and raising the arch [4,7]. If the plantar fascia is sufficiently stiff to remain isometric, MTPJ dorsiflexion should be directly coupled to arch deformation (figure 1). However, the extensibility of the plantar fascia could influence the arch shape changing effect of the windlass mechanism. If the plantar fascia elongates or shortens simultaneously to the windlass mechanism, it could, respectively, reduce or increase the magnitude of arch deformation relative to the pure windlass mechanism. Analogously, pulling a weight (the calcaneus) with an elongating elastic band produces less motion than pulling it with a steel rope.

During both walking and running gaits, there is evidence that the plantar fascia strains during mid- to late stance [7–13], simultaneously to MTPJ dorsiflexion and arch rise, and thus the forward-windlass mechanism [4,7,8,14]. We question if the straining plantar fascia compromises the one-to-one coupling between arch deformation and toe arc length change from MTPJ dorsiflexion during running (figure 1). Addressing this question is challenging because plantar fascia strain is difficult to measure during locomotion. While current approaches such as motion capture [7–10], ultrasound [7,9,10] and single plane fluoroscopy [12,13] have provided insight into plantar fascia and foot function, they do not capture the three-dimensional motions of individual bones within the foot during locomotion. Using three-dimensional biplanar videoradiography, we modelled plantar fascia elongation using subject-specific bone motion in addition to MTPJ dorsiflexion as a proxy for an engaged windlass mechanism. We investigate the timing of the extensibility of the plantar fascia and discuss how deviations from a pure windlass mechanism may affect arch function in running.

2. Methods

(a) Experimental set-up and subject characteristics

Running data were pooled from three datasets that use X-ray reconstruction of moving morphology (XROMM), a three-dimensional imaging technology for visualizing rapid skeletal movement *in vivo* [15,16]. The combined subject pool comprised 12 participants (8M, 4F; mean ± s.d.: height 1.69 ± 0.06 m, weight 70 ± 12 kg). Two datasets (11 subjects) were collected at the Brown University Keck Facility (Brown University, USA). One subject's data were collected at the Skeletal Observation Lab using a similar biplanar videoradiography system (see electronic supplementary material, figure S1 for visual methods flowchart) (Queen's University, Canada).

(b) Data collection: computed tomography scans of the right foot

Computed tomography (CT) scans were taken of each participant's right foot while they were prone (model: Lightspeed 16, $n = 11$; Revolution HD, $n = 1$; General Electric Medical Systems, USA). Seven participants received their scan with the plantar surface of their foot constrained at 90° from the scanning table (average resolution: 0.577 × 0.577 × 0.625 mm) and five participants were scanned with their foot in a prone position to increase the resolution (average resolution: 0.393 × 0.393 × 0.625 mm). The tibia, calcaneus, first metatarsal, first proximal phalanx and sesamoids were segmented (Mimics, Materialise, Leuven, Belgium). Partial volumes were generated to create digitally reconstructed radiographs [17]. Tessellated meshes

representing the bone surfaces were also created from the CT scans. Inertial anatomical coordinate systems were generated from the bone meshes, with the origin located at the centroid and the x–y–z axes aligned along the principal axes of the moment of inertia tensor [18]. The axes were re-labelled such that the x-axis was lateral, the y-axis was anterior and the z-axis was superior.

(c) Data collection: biplanar videoradiography of running

Participants in all collections were instructed to run barefoot at a self-selected speed and strike pattern along a raised walkway. They were allowed as much time as required to become familiar with the raised walkway and with the selected starting position, which ensured that the participant's right foot landed naturally in the middle of the X-ray volume. Three barefoot running trials were collected using biplanar videoradiography (250 Hz, range of 70–80 kV, 100–125 mA). One trial from each participant was selected for analysis, guided by X-ray image quality.

(d) Data processing: kinematics derived from biplanar videoradiography

The processing pipeline for foot biplanar videoradiography data has been described previously [19]. Briefly, the high-speed cameras were calibrated using a custom calibration object and the images were undistorted [15], using X-ray-specific software [16] (XMALab, Brown University, USA). The orientation and translation of the tibia, calcaneus, first metatarsal and first proximal phalanx were measured by markerlessly tracking the digitally reconstructed radiographs using custom software [17] (Autoscoper, Brown University, USA). All of the sesamoid bones inferior to the first metatarsal were tracked as a single rigid body, but due to bone occlusion, it was difficult to track all six degrees of freedom. The rotation of the phalanx was used as a starting point, as the sesamoid–phalangeal ligament apparatus is quite stiff [20], and probably rotates similarly about the metatarsal head. The sesamoid unit was then purely translated to best fit the X-ray images.

Gait events were defined using kinematic trajectories of specified inferior points on each bone surface. The strike pattern was classified as either fore-foot strike (FFS) or rear-foot strike (RFS) from the X-ray images. Initial contact was defined as the instant that either the sesamoids (for FFS) or calcaneus (for RFS) contacted the ground. The heel and fore-foot contact were defined as the instant of maximum negative vertical velocity. Physically, this is the point where the contact with the ground causes the acceleration vector to change direction, and would mimic the instant the ground reaction force registers. Toe-off was defined by manually selecting the frame where the toes were not in contact with the ground.

The inertial axes computed from the surface meshes defined the anatomical coordinate systems for the tibia, calcaneus, first metatarsal and first proximal phalanx [18]. The coordinate system axes were re-labelled such that the x-, y- and z-axes more closely represented dorsiflexion, inversion and adduction, respectively, with reference to the right foot. A ZYX Tait–Bryan angle sequence determined the angles of the first metatarsal relative to the calcaneus (arch angles) and the phalanx relative to the metatarsal (MTPJ angle). To simplify our description of arch motion, we refer to arch flattening as a combination of arch dorsiflexion and abduction, and arch rise as the combination of arch plantarflexion and adduction. The arch angular velocity is the resultant three-dimensional angle of rotation around the instantaneous helical axis of the first metatarsal relative to the calcaneus, computed between every frame, differentiated with respect to time. All angles were filtered with an adaptive low-pass Butterworth filter with a cut-off frequency between 10 and 20 Hz, depending on the signal content at each time point [21]. This filter preserves more of the high-frequency signal content during the impact event at initial contact than a conventional low-pass Butterworth filter with a cut-off frequency of 10 Hz.

(e) Plantar fascia modelling

The plantar fascia was modelled as two fibres connecting the origin and the insertion of the first slip of the plantar fascia. The origin was selected as two points on the medial one-fifth (i.e. the medial side of the plantar fascia tissue) of the lateral tubercle of the calcaneus, and the insertion was selected on the medial and lateral insertion points of the phalanx for one subject [5,22]. The bones of all other subjects were aligned using the inertial anatomical coordinate systems and a coherent point drift algorithm ensured that the origins and insertions were placed consistently among subjects [23]. The plantar fascia fibre connected the selected origin and insertion, with the constraint that the fibre cannot pass through any bone. Using generated distance fields for each bone, a custom optimization was implemented using the sequential quadratic programming routine with fmincon in MATLAB (R2019a, Mathworks, USA), with 100 points used for each fibre [24]. A convex hull was created around the sesamoids to model the inter-sesamoid ligaments and to prevent the fibre from falling between them. The optimization algorithm was given an initial guess using guiding points on the inferior side of sesamoid, which then converged to optimal solutions around the sesamoids. The optimal solution was also visually verified. The lengths of these two fibres were measured as the sum of the Euclidean distances between adjacent points. The elongation of the fibres was normalized to the longest plantar fascia length in the trial. The normalized elongation was filtered with an adaptive low-pass Butterworth filter with a cut-off frequency between 10 and 20 Hz [21].

(f) Classification of plantar fascia behaviour

We describe the effect of the plantar fascia's extensibility on the windlass mechanism by examining the coupling between MTPJ rotation and plantar fascia elongation during stance phase. We examined the time-series curves qualitatively, and then quantified our observations by selecting a threshold change in MTPJ rotation and plantar fascia elongation that we considered quasi-constant. We classified each 1% of stance into phases using our selected thresholds, which equate to less than 2% of the range of each variable. Specifically, if the MTPJ angle change was less than 0.5°, it was classified as quasi-constant. If the MTPJ angle change was larger than 0.5° and positive, the MTPJ was classified as dorsiflexing, while if it was larger than 0.5° and negative, the MTPJ was classified as plantarflexing. Similarly, if the plantar fascia underwent less than 0.0005 normalized elongation between each percentage of stance, it was classified as quasi-isometric. If it was larger than 0.0005 and positive, the plantar fascia was elongating; if it was larger than 0.0005 and negative, the plantar fascia was shortening. The thresholds were selected to visually correspond with the mean time-series curves and then applied to each participant's individual data. We conducted a sensitivity analysis on our classification paradigm, altering each threshold by ±20% and ±40% while keeping the other variable at the selected threshold.

Consideration of a windlass mechanism that accounts for an extensible plantar fascia requires a more detailed framework than originally described by Hicks. During periods where there is minimal elongation of the plantar fascia, the reverse-windlass occurs if the MTPJ plantarflexes while the arch flattens, and the pure forward-windlass occurs if there is dorsiflexion at the MTPJ and simultaneous arch rising. If the plantar fascia elongates during MTPJ dorsiflexion, it may inhibit arch deformation compared with the pure forward-windlass, and thus

we term it an inhibited forward-windlass mechanism. Alternatively, if the plantar fascia shortens simultaneously to MTPJ dorsiflexion, it may enhance arch rising compared with the pure forward-windlass, as both the shortening plantar fascia and the windlass mechanism act to raise the arch. Thus, we term this phase an enhanced forward-windlass mechanism.

To quantify deviations from the windlass mechanism in the sagittal plane resulting from an extensible plantar fascia, we tested a simple model. The original description of the windlass mechanism states that the arc length change around the MTPJ (Δs) should be directly coupled with arch length change (Δl) [4] (figure 1). The MTPJ arc length change (Δs) is measured as the product of the radius of the metatarsal head (r) and MTPJ angle change per 1% of stance ($\Delta\theta$). The radius of the metatarsal head (r) was measured as the radius of a least-squares sphere fit to the bone mesh vertices. The arch length was measured as the three-dimensional distance between an inferior point on both the calcaneus and the metatarsal, and the change in arch length was measured between every 1% of stance. The change in MTPJ arc length was subtracted from the change in arch length. If positive, this indicates that the arch is shortening more than predicted by the ideal windlass (enhanced windlass); if negative, it is less than predicted by the ideal windlass (inhibited windlass); or if close to 0, it is equivalent to an ideal windlass. The mean arch length change is computed in the inhibited, pure and enhanced forward-windlass phases as classified by the phase analysis.

3. Results

(a) Metatarsal–phalangeal joint, arch and plantar fascia behaviour during the stance phase of running

MTPJ dorsiflexion, plantar fascia elongation, arch angles and the magnitude arch angular velocity were generally similar among subjects regardless of strike pattern (figures 2 and 3). We describe stance phase in three sections: early stance, mid-stance and propulsion, divided to approximately coincide with mean MTPJ motion (figure 4*a*).

During early stance (0 to approx. 20%), the MTPJ primarily plantarflexed, during which the plantar fascia generally shortened or remained quasi-isometric before beginning to lengthen closer to mid-stance (figure 4). Arch dorsiflexion and abduction occur quickly during this time (figure 2), as evidenced by the high magnitude of arch angular velocity. The initial quasi-isometric plantar fascia during MTPJ plantarflexion with arch flattening is consistent with a reverse-windlass mechanism (figure 4*c*).

During mid-stance (approx. 20% to approx. 55%), the MTPJ angle changed minimally when the toes were flat on the floor (figure 4). The plantar fascia elongated at the beginning of this phase for 11 of the 12 participants, with some participants experiencing plantar fascia elongation throughout mid-stance, while others experienced a phase of minimal plantar fascia elongation. None of the participants had plantar fascia shortening. The arch continued to dorsiflex and abduct, but more slowly than in early stance.

In propulsion (approx. 55% to approx. 85%), the MTPJ dorsiflexed after heel lift, with half of the participants experiencing a combined MTPJ dorsiflexion and plantar fascia elongation phase (inhibited forward-windlass) (figure 4). All participants then underwent a pure forward-windlass phase, with a quasi-isometric plantar fascia and MTPJ dorsiflexion. However, there was variability among participants in the amount of time spent in this phase. After the pure forward-windlass phase, there was a consistent enhanced forward-windlass phase, in which the MTPJ continued to dorsiflex while the plantar fascia shortened. Arch velocity was high in this phase, with the arch plantarflexing and adducting.

The theoretical behaviour of the windlass mechanism, in which MTPJ arc length change is coupled with arch length change, shows a similar pattern to the inhibited-pure-enhanced sequence of the forward-windlass mechanism (figure 5). During the inhibited forward-windlass mechanism, there is less arch shortening than would be expected during the pure forward-windlass phase. Additionally, there is more arch shortening when the plantar fascia shortens concurrently to the forward-windlass mechanism, suggesting that there is an enhanced forward-windlass phase.

Immediately before toe-off, all but one participant with the foot in view of the X-ray system experienced MTPJ plantarflexion and plantar fascia shortening.

(b) Arch ligament behaviour during initial contact

We found that plantar fascia elongation consistently occurred later than 15–20% of stance, and that the load of impact on the arch may be managed in the earlier MTPJ plantarflexion phase, where the plantar fascia is most often shortening or remaining quasi-isometric (reverse-windlass). We postulated that the large amount of arch flattening during the reverse-windlass action is likely slowed by the loading of tissues proximal to the plantar fascia, which have been shown to absorb and return strain energy [3]. To investigate the elongation timing of the proximal ligaments, we used data from one participant with additional tracked bones. Three of the proximal ligaments (the spring ligament, the short plantar ligament and the deep fibres of the long plantar ligament) were modelled with the same algorithm as the plantar fascia (electronic supplementary material, methods S2, figure S2). The elongation profile of the plantar ligaments and the medial component of the spring ligament matched the participant's arch dorsiflexion profile, supporting the idea that the proximal arch ligaments could be managing more of the initial load on the arch (figure 6).

4. Discussion

Our experimental results show that the plantar fascia dynamically shifts its behaviour during running gait. At initial contact, the plantar fascia does not elongate, suggesting that MTPJ plantarflexion and the reverse-windlass mechanism may allow arch-spanning tissues to mitigate more of the load of impact than the plantar fascia. This eliminates the need for the plantar fascia to directly elongate to slow arch deformation. In propulsion, the pure forward-windlass raises the arch with a quasi-isometric but highly elongated plantar fascia, which would delay the return of the plantar fascia's strain energy until later in stance. The shortening plantar fascia and forward-windlass mechanism then may work in tandem to shorten the arch. These findings elucidate the influence and timing of the extensible plantar fascia on the windlass mechanism during running gait.

Our data show that in early stance, the plantar fascia does not elongate substantially until arch flattening has already slowed; instead, the plantar fascia facilitates the reverse-windlass motion of the foot, probably so that proximal arch ligaments manage the load before the plantar fascia. The arch dorsiflexion curves and the elongation profiles of the

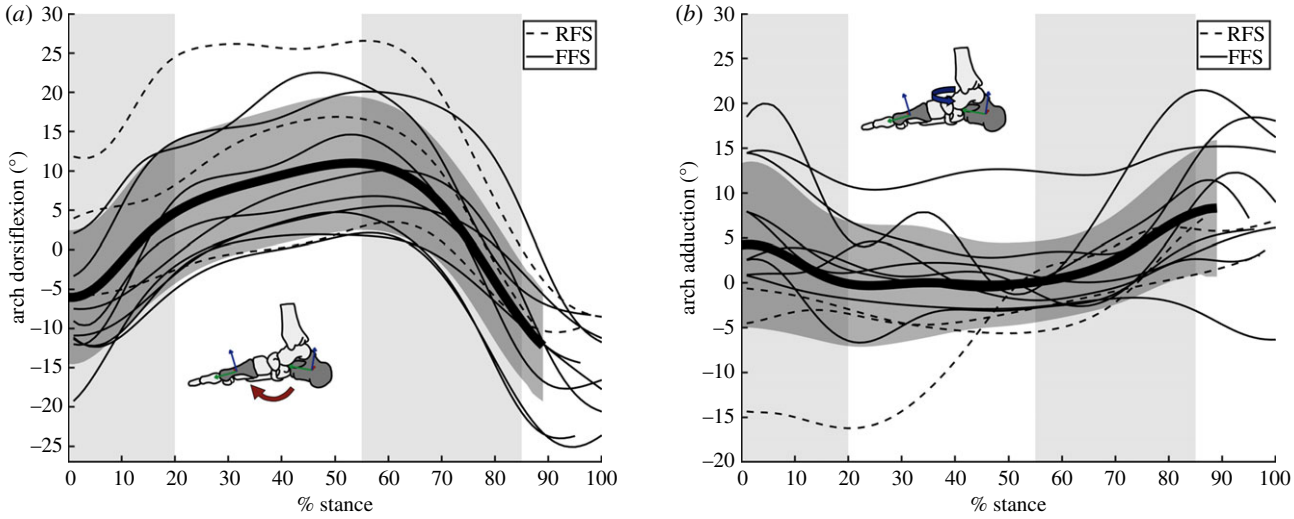

Figure 2. Arch angles. The (*a*) dorsiflexion and (*b*) adduction angle between the first metatarsal and the calcaneus during running stance phase. The thickest line and dark grey region represent the mean ± 1 s.d. The subject's strike pattern is indicated with either a dashed (rear-foot strike, RFS) or solid (fore-foot strike, FFS) line. The light grey shaded regions highlight early stance (0–20%), mid-stance (20–55%) and propulsion (55–85%) to facilitate comparison with figure 4. (Online version in colour.)

proximal arch ligaments are similar while the plantar fascia shortens or remains quasi-isometric. This timing suggests that the arch ligaments might contribute more strain energy absorption to the arch-spring than the plantar fascia during early stance; however, we cannot confirm this without measures of force in the arch-spanning tissues. Further, if MTPJ dorsiflexion is limited before initial contact, inhibiting the reverse-windlass, the distribution of load among arch tissues could be altered. Thus, certain types of footwear (e.g. the reinforced toe box in many shoes) or foot pathologies like hallux rigidus, for example, could modify the distribution of energy absorption across the arch.

For half of the participants, there were periods when the windlass effect on the arch may have been inhibited by the elongating plantar fascia. The arch shortened less, and more slowly, at the beginning of propulsion when these participants were in an inhibited forward-windlass phase than when they were in a pure or enhanced forward-windlass phase. This could be an indication that the Achilles tendon force on the calcaneus was higher than the combined resistance of the passive arch tissues and the intrinsic foot muscles. Inter-subject variation in passive tissue stiffness or intrinsic foot muscle activation may be responsible for the existence of an inhibited forward-windlass phase. While we cannot measure whether the inhibited forward-windlass inhibits arch deformation with our approach, it warrants further study to explain the variability among participants in the time spent in this phase, or if they entered the phase at all.

We consistently saw a pure forward-windlass phase in propulsion where the plantar fascia was quasi-isometric while the MTPJ experienced substantial dorsiflexion, and the arch rose. There were variations in the time spent in this phase, but the arch length change was coupled to the arc length change expected from MTPJ dorsiflexion about the metatarsal head, suggesting that the windlass mechanism as Hicks originally described it is generally present during running gait [4]. The plantar fascia's role through the forward-windlass in propulsion is to resist the tendency of the mid-foot to break in response to the body's weight, such that the foot becomes a stable base of support, but not a rigid lever [4,25]. If the mid-foot was breaking after heel rise, we would see additional arch flattening (or arch dorsiflexion). However, we see substantial arch rising, comprising arch plantarflexion and adduction. Our data suggest, therefore, that the forward-windlass and the plantar fascia contribute to stabilizing the foot, by counteracting mid-foot break. However, there is substantial motion that occurs in the arch during this phase, which conflicts with the description of the foot as a rigid lever, as has been recently questioned by several researchers [14,25]. While this study lacks kinetic data to measure dynamic stiffness of the arch, previous studies have shown that the windlass mechanism does not stiffen the foot [26–28], and that the arch is more compliant in late stance than in the first half of stance [14]. Therefore, we propose that the arch complex is best described as a dynamic lever rather than a rigid lever, as it provides a stable base of support for push-off, with a constantly changing lever arm.

The plantar fascia prevents mid-tarsal break through high tension in propulsion, but does so at a quasi-isometric length, which delays the return of stored strain energy to the arch. The quasi-isometric length during the pure forward-windlass phase suggests that tension in the plantar fascia is relatively constant, while the ankle has already started to plantarflex and generate power [14]. The mechanism that mediates this prolonged quasi-isometric behaviour cannot be deduced without measures of forces acting on the foot. However, it seems likely that after this period, the rapid shortening of the plantar fascia would contribute to arch power generation as the arch is rising rapidly and generating positive power during this phase of gait [14]. We speculate that through a fine-tuned balance of the extrinsic and intrinsic muscle forces as the toes move into dorsiflexion, the plantar fascia's strain energy is maintained from approximately 55–70% of stance, such that it can then contribute to arch power in late stance, during the enhanced forward-windlass. This could compensate for the positive power reduction at the ankle, which occurs at a temporally similar time to the transition between the ideal and enhanced forward-windlass phases. Alternatively, the conversion of absorbed energy at the MTPJs, partially resulting from intrinsic foot muscles [29], to positive arch power by the plantar fascia [8,9], could be facilitated with an isometric plantar fascia, by reducing the energy dissipation that would occur with tissue shortening.

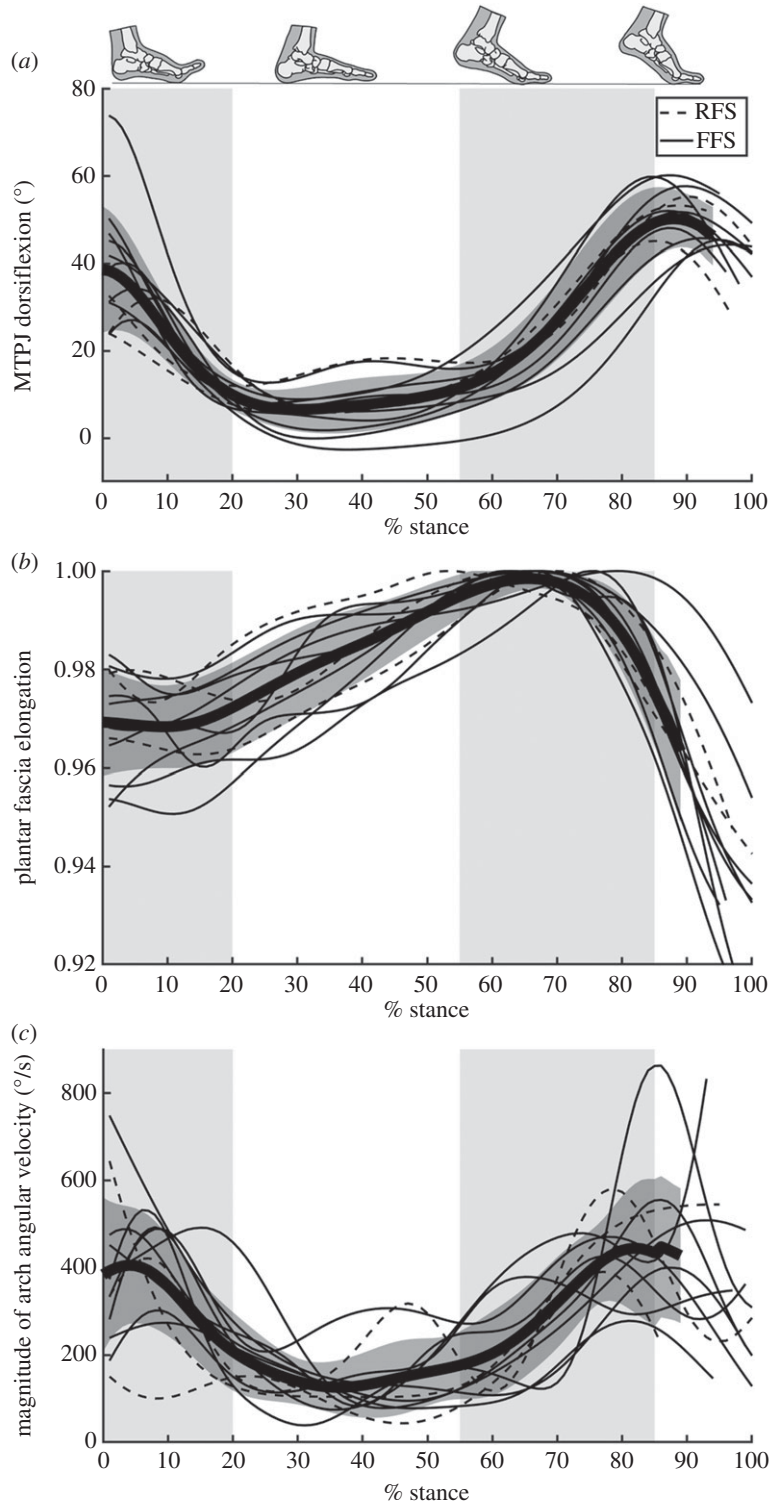

Figure 3. MTPJ angle, plantar fascia elongation and magnitude of arch angular velocity. (*a*) MTPJ dorsiflexion, (*b*) plantar fascia elongation and (*c*) the magnitude of 3D arch angular velocity over the stance phase of running gait. The thickest line and dark grey region represent the mean ± 1 s.d. The subject's strike pattern is indicated with either a dashed (rear-foot strike, RFS) or solid (fore-foot strike, FFS) line. The light grey shaded regions highlight early stance (0–20%), mid-stance (20–55%) and propulsion (55–85%) to facilitate comparison with figure 4.

However, while our data are consistent with these concepts, we cannot directly measure these ideas with our approach.

Our plantar fascia elongation values are consistent with existing data; however, we did not observe consistent differences in running strike patterns, and we measured a later time of peak strain. The plantar fascia strain values here match the work of Wager & Challis [9], with an average peak strain around 6% and initial contact strain around 4%. McDonald *et al*. [8] found a similar 2% strain from initial contact to maximum strain, but selected a smaller resting length, leading to lower initial strain values. Early stance pre-loading of the plantar fascia has been shown in running, and is significantly higher in rear-foot strike participants [8,9]. While we unfortunately do not have the statistical power to make inferences between strike patterns, and our distribution of rear-foot strikers and fore-foot strikers was skewed (3 : 9), the plantar fascia of the rear-foot strikers was not consistently more strained at heel strike. Further, several

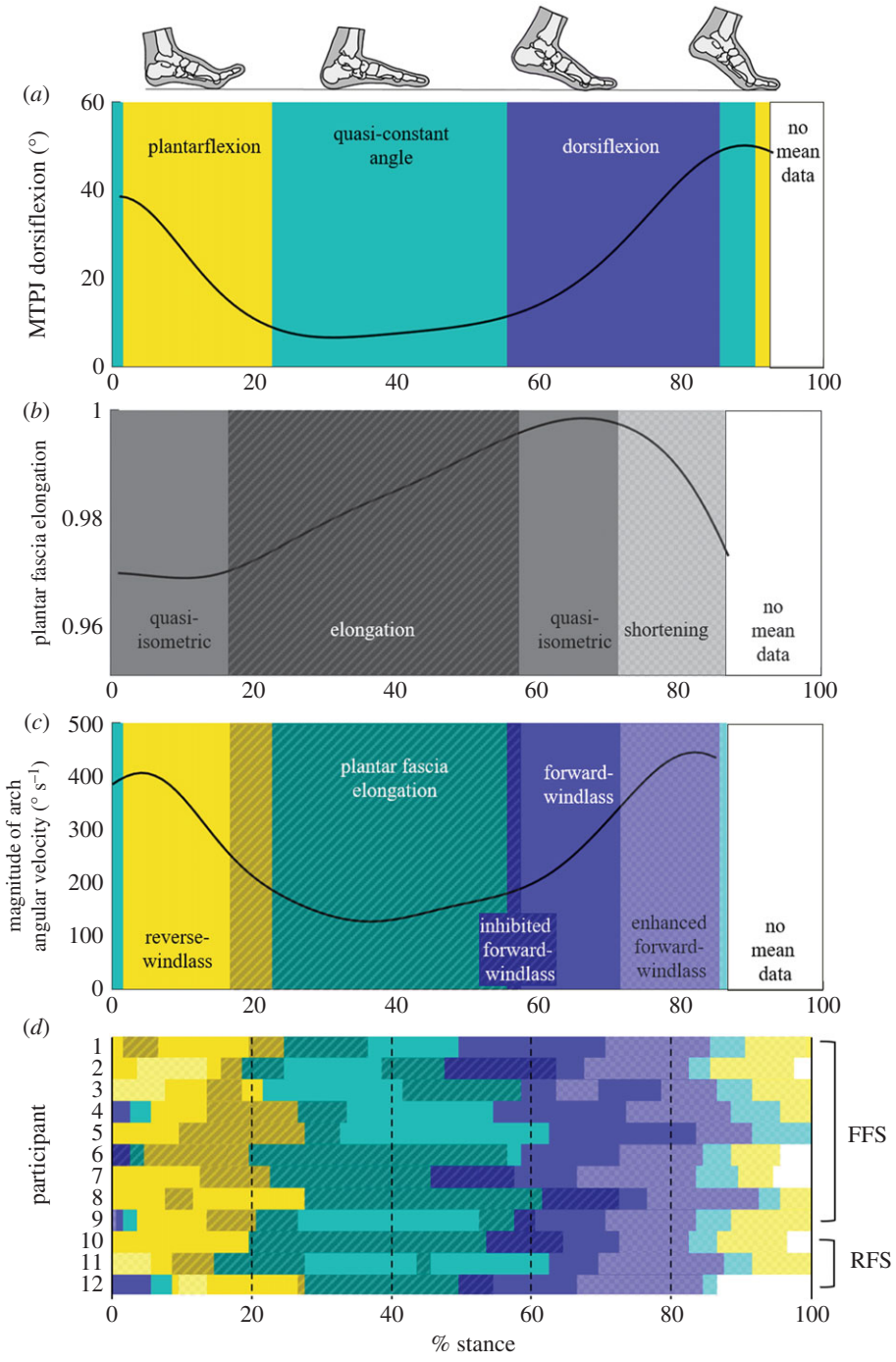

Figure 4. Classification of windlass mechanism phases. (*a*) The mean of all participants' metatarsophalangeal joint (MTPJ) angle is classified into phases based on whether it is plantarflexing (yellow, light), staying within the 0.5° per 1% stance threshold as quasi-constant (teal, medium), or dorsiflexing (purple, dark). (*b*) The plantar fascia elongation is classified as elongation (dark diagonal lines), staying within the 0.0005 normalized elongation per 1% of stance threshold as quasi-isometric (no pattern), or shortening (light checkerboard). (*c*) The magnitude of the three-dimensional arch angular velocity is super-imposed over the classification of windlass mechanism behaviour. The plantar fascia elongation phases in (*b*) are matched with the windlass engagement (MTPJ dorsiflexion) periods in (*a*) to highlight the phases of inhibited, pure or enhanced forward-windlass, as well as the reverse-windlass phase. (*d*) The phases for each participant using the same thresholds as were selected for the mean MTPJ angle and plantar fascia elongation.

participants, regardless of strike pattern, had some form of plantar fascia shortening at initial contact, which has only been shown for RFS patterns [8]. The time of peak strain was also later in our work compared with published values (67 ± 6% of stance compared with approx. 60% [8,9]). These variations could be a result of methodological differences between motion capture and biplanar videoradiography technology, or (more likely) due to our inclusion of the sesamoid bones, which increase the moment arm around the metatarsal head by close to half the diameter for some subjects. Variations in the sesamoids' position during gait can change the direction of the force applied to the first metatarsal and maintain strain in the plantar fascia.

The thresholds in the analysis of windlass mechanism timing and plantar fascia elongation were selected subjectively based on visual assessment of the time-series curves. We modified each threshold by ±20% and ±40%, keeping the other at the selected value (0%), to determine the sensitivity of our results to the threshold values. The order of the phases changed minimally, while the time spent in

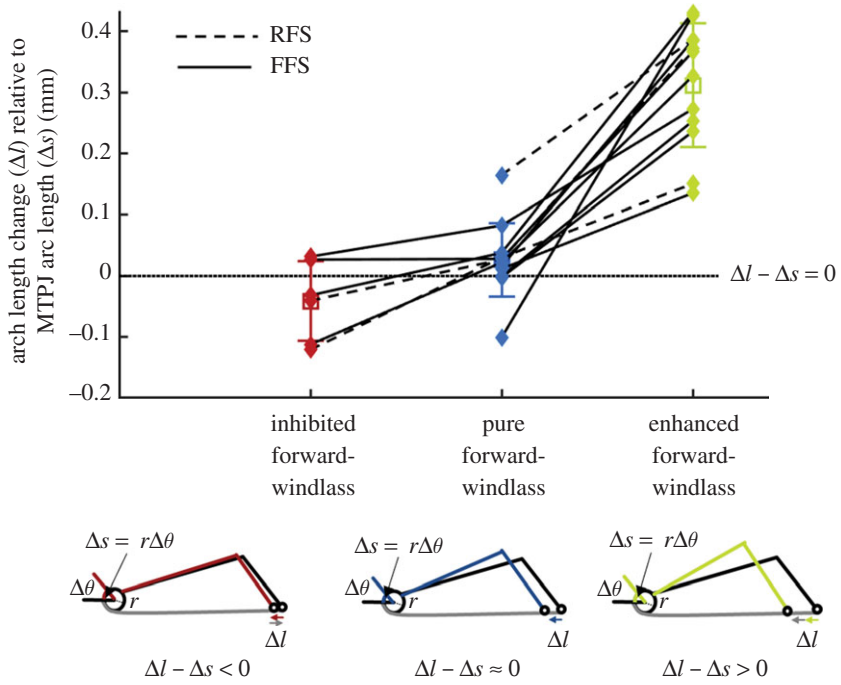

Figure 5. Windlass mechanism coupling with arch length change. For the pure forward-windlass mechanism, as the MTPJ dorsiflexes, the change in arc length (Δs) should be equal to the change in the length of the arch (Δl), such that the difference between them is 0 (i.e. $\Delta l - \Delta s = 0$). The difference between arch length change and MTPJ arc length change is averaged during the phases as classified in figure 4. There is reduced arch length change during the inhibited forward-windlass, and additional arch length change in the enhanced forward-windlass compared with the same participant's pure forward-windlass mechanism, as indicated by connecting lines (dashed, rear-foot strike, RFS; solid, fore-foot strike, FFS). (Online version in colour.)

each phase varied. As the thresholds were increased, as expected, all quasi-constant phases lengthened. Thus, when the plantar fascia elongation threshold increased, the pure forward-windlass phase lengthened, while the inhibited forward-windlass phase shortened because the plantar fascia elongation that was originally coded as elongation changed to a quasi-isometric phase. Furthermore, as the MTPJ angle threshold increased, the quasi-constant angle phase lengthened, reducing the MTPJ dorsiflexion phase. The overall time available for any forward-windlass phase was thus reduced, consequently shortening the inhibited and enhanced forward-windlass phases. When the MTPJ threshold was decreased by 20%, an additional participant experienced the inhibited forward-windlass phase, while a different participant no longer had an inhibited forward-windlass phase when the threshold was increased by 40%. The plantar fascia elongation threshold played a bigger role at initial contact than the MTPJ threshold change. As the plantar fascia elongation threshold decreased, the pure reverse-windlass phase had plantar fascia shortening as well. This indicates that the foot may not always have a pure reverse-windlass mechanism; however, it does not change our interpretation of limited plantar fascia elongation at initial contact, in favour of the elongation of more proximal arch ligaments. Overall, these changes do not influence our interpretations as there is clear variability among subjects regardless, and we assess primarily the existence, order and potential significance of the phases. Future work is required to understand variation in the length of the phases, and whether the plantar fascia and windlass mechanism are responsible for the variations in arch deformation seen here.

There is inter-subject variability in the phase presence and timing, which may be derived from several sources. We were unable to measure running speed accurately during the trials as we only have distal tibia and foot kinematic data. We probably have differences in running speed among subjects, supported by the range of contact times from 0.22 to 0.37 s, which could represent variations of Froude numbers from 0.3 to 1.6 [30]. We estimated the participants' leg lengths using the proportion of 48.5% of their stature and found a group mean estimate of speed of 3.4 m s^{-1} (range: 3.0–3.8 m s^{-1}) [31]. These differences are due to the short runway length in 11 out of 12 of the subjects' collections. We also selected only one trial from every participant and as a result, we are unable to determine whether these trials were representative of their typical running patterns, nor assess the within-subjects' variability in the timing of the windlass phases. Furthermore, we restricted our analysis to the medial slip of the plantar fascia and the first ray of the foot primarily due to the difficulty in measuring the dynamic motion of the other metatarsals. While we deemed this a reasonable assumption as the medial segment of the plantar fascia is the most strained during walking [7], the plantar fascia's central and lateral band, as well as the inter-metatarsal ligaments play a role in the stiffness and support of both the medial and the transverse arches, and their influence could vary based on the participant [32]. The resting length of the plantar fascia is also unknown, and may explain some variation in plantar fascia elongation. It is unclear if the plantar fascia is completely slack at any point during gait, and whether it goes slack could be dependent on the participant. During running gait, MTPJ dorsiflexion probably tensions the plantar fascia before initial contact [33,34], possibly so that it is no longer in the toe region of its force-elongation curve. If the plantar fascia was slack or bearing low tension at initial contact, we would expect it to strain substantially when the foot is loaded; however, we saw plantar fascia shortening or quasi-isometric behaviour. In late

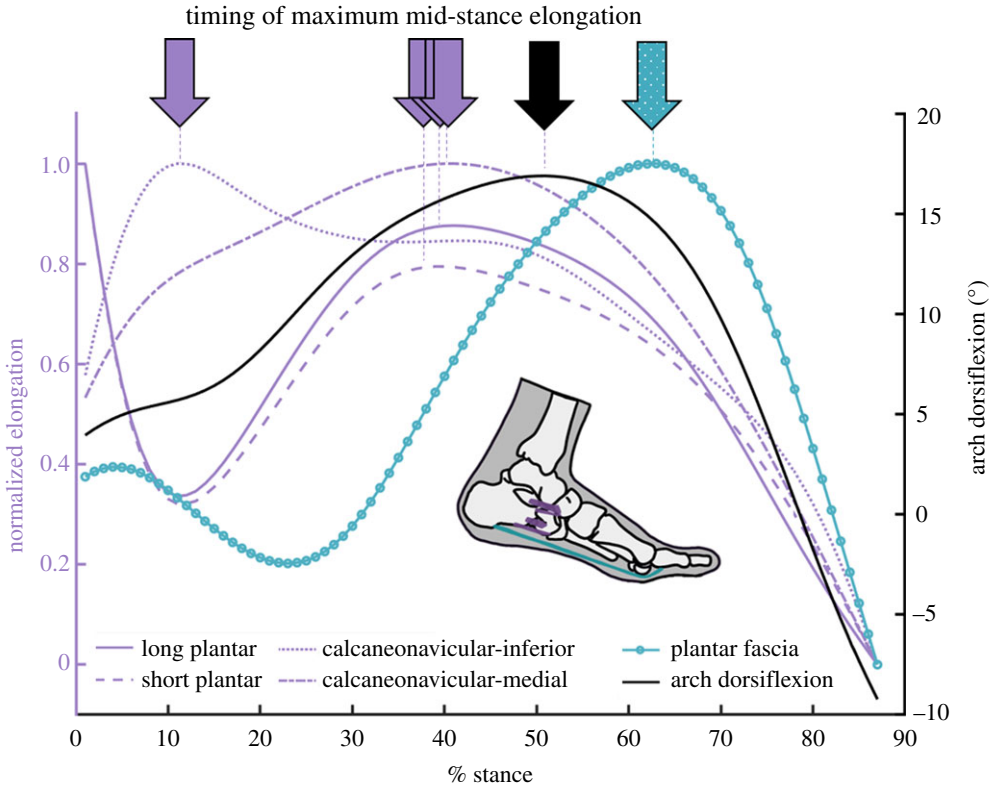

Figure 6. Arch ligament deformation. The arch dorsiflexion over the stance phase of running (black, right *y*-axis) shows similar maximum timing to the elongation of the arch-spanning ligaments. Elongation of the arch-spanning ligaments normalized to the range of elongation are measured on the left *y*-axis (purple). The plantar fascia's normalized elongation is measured on the left *y*-axis but is shown in teal dots to highlight the later peak elongation. (Online version in colour.)

stance, the plantar fascia shortens well below the strain at initial contact and could be the plantar fascia going slack for some participants. To minimize errors from selecting a slack length, we normalized to the subject-specific maximum plantar fascia length.

In conclusion, we have described the influence of the extensibility of the plantar fascia on the windlass mechanism. Our findings show that the extensibility of the plantar fascia plausibly can inhibit or enhance the forward-windlass mechanism's effect on arch deformation. Overall, this work suggests that the plantar fascia plays a central role in managing the foot–ground interaction during locomotion, which may highlight why the plantar fascia is thicker and more pronounced in terrestrial hominins compared with more arboreal primates [35,36]. Furthering our understanding of the complex behaviour of the foot will probably have additional important applications, such as influencing therapies in podiatry, orthopaedics and physical therapy as well as improving the anatomical basis in the design of shoes, prostheses and biomimetic robots.

Ethics. Experimental protocols were approved by the Providence VA Medical Center Institutional Review Board, the Brown University Institutional Review Board or Queen's University Health Sciences & Affiliated Teaching Hospitals Research Ethics Board. All subjects gave informed consent prior to participation in the data collection.

Data accessibility. Data and MATLAB code for the figures in the manuscript and electronic supplementary material are available from the Dryad Digital Repository: https://doi.org/10.5061/dryad.v9s4mw6sz [37].

Authors' contributions. L.W. and M.J.R. conceived the analysis, with input from L.A.K. and G.A.L. All authors contributed to data collection and processing. L.W. analysed the data with assistance from M.J.R. L.W. and M.J.R. wrote the manuscript with help from L.A.K. and G.A.L. L.W., L.A.K., G.A.L., D.E.L. and M.J.R. edited the manuscript. All authors approved the final version.

Competing interests. The authors declare no competing interests.

Funding. This project was funded by the Australian Research Council (ARC) Discovery grant no. (DP160101117), the NSERC Discovery grant no. (RGPIN/04688-2015) and the NSERC Postgraduate Doctoral Scholarship. It was also supported by a Congress Travel Grant from the International Society of Biomechanics.

Acknowledgements. The authors would like to thank Dr Dominic Farris for his insights on an early draft of the manuscript.

References

1. D'Août K, Aerts P. 2008 *The evolutionary history of the human foot*. Maastricht, The Netherlands: Shaker Publishing.
2. Holowka NB, Lieberman DE. 2018 Rethinking the evolution of the human foot: insights from experimental research. *J. Exp. Biol.* **221**, jeb174425. (doi:10.1242/jeb.174425)
3. Ker RF, Bennett MB, Bibby SR, Kester RC, Alexander RMcN. 1987 The spring in the arch of the human foot. *Nature* **325**, 147–149. (doi:10.1038/325147a0)
4. Hicks JH. 1954 The mechanics of the foot. II. The plantar aponeurosis and the arch. *J. Anat.* **88**, 25–30.
5. Bojsen-Moller F, Flagstad KE. 1976 Plantar aponeurosis and internal architecture of the ball of the foot. *J. Anat.* **121**, 599–611.
6. Stearne SM, McDonald KA, Alderson JA, North I, Oxnard CE, Rubenson J. 2016 The foot's arch and the energetics of human locomotion. *Sci. Rep.* **6**, 19403. (doi:10.1038/srep19403)

7. Caravaggi P, Pataky T, Goulermas JY, Savage R, Crompton R. 2009 A dynamic model of the windlass mechanism of the foot: evidence for early stance phase preloading of the plantar aponeurosis. *J. Exp. Biol.* **212**, 2491–2499. (doi:10.1242/jeb.025767)
8. McDonald KA, Stearne SM, Alderson JA, North I, Pires NJ, Rubenson J. 2016 The role of arch compression and metatarsophalangeal joint dynamics in modulating plantar fascia strain in running. *PLoS ONE* **11**, e0152602. (doi:10.1371/journal.pone.0152602)
9. Wager JC, Challis JH. 2016 Elastic energy within the human plantar aponeurosis contributes to arch shortening during the push-off phase of running. *J. Biomech.* **49**, 704–709. (doi:10.1016/j.jbiomech.2016.02.023)
10. Caravaggi P, Pataky T, Günther M, Savage R, Crompton R. 2010 Dynamics of longitudinal arch support in relation to walking speed: contribution of the plantar aponeurosis. *J. Anat.* **217**, 254–261. (doi:10.1111/j.1469-7580.2010.01261.x)
11. Erdemir A, Hamel AJ, Fauth AR, Piazza SJ, Sharkey NA. 2004 Dynamic loading of the plantar aponeurosis in walking. *J. Bone Joint Surg. Am.* **86**, 546–552.
12. Fessel G, Jacob HAC, Wyss C, Mittlmeier T, Müller-Gerbl M, Büttner A. 2014 Changes in length of the plantar aponeurosis during the stance phase of gait—an in vivo dynamic fluoroscopic study. *Ann. Anat. Anat. Anz. Off. Organ Anat. Ges.* **196**, 471–478. (doi:10.1016/j.aanat.2014.07.003)
13. Gefen A. 2003 The in vivo elastic properties of the plantar fascia during the contact phase of walking. *Foot Ankle Int.* **24**, 238–244. (doi:10.1177/107110070302400307)
14. Bruening DA, Pohl MB, Takahashi KZ, Barrios JA. 2018 Midtarsal locking, the windlass mechanism, and running strike pattern: a kinematic and kinetic assessment. *J. Biomech.* **73**, 185–191. (doi:10.1016/j.jbiomech.2018.04.010)
15. Brainerd EL, Baier DB, Gatesy SM, Hedrick TL, Metzger KA, Gilbert SL, Crisco JJ. 2010 X-ray reconstruction of moving morphology (XROMM): precision, accuracy and applications in comparative biomechanics research. *J. Exp. Zool. Part Ecol. Genet. Physiol.* **313**, 262–279. (doi:10.1002/jez.589)
16. Knörlein BJ, Baier DB, Gatesy SM, Laurence-Chasen JD, Brainerd EL. 2016 Validation of XMALab software for marker-based XROMM. *J. Exp. Biol.* **219**, 3701–3711. (doi:10.1242/jeb.145383)
17. Miranda DL, Schwartz JB, Loomis AC, Brainerd EL, Fleming BC, Crisco JJ. 2011 Static and dynamic error of a biplanar videoradiography system using marker-based and markerless tracking techniques. *J. Biomech. Eng.* **133**, 121002. (doi:10.1115/1.4005471)
18. Eberly D, Lancaster J, Alyassin A. 1991 On gray scale image measurements: II. Surface area and volume. *CVGIP Graph. Models Image Process.* **53**, 550–562. (doi:10.1016/1049-9652(91)90005-5)
19. Kessler SE, Rainbow MJ, Lichtwark GA, Cresswell AG, D'Andrea SE, Konow N, Kelly LA. 2019 A direct comparison of biplanar videoradiography and optical motion capture for foot and ankle kinematics. *Front. Bioeng. Biotechnol.* **7**, 199. (doi:10.3389/fbioe.2019.00199)
20. Sarrafian S. 1993 Proximal phalangeal apparatus of the big toe. In *Anatomy of the foot and ankle* (eds D Patterson, M Dickmeyer, E Durand), pp. 211–214. Philadelphia, PA: JB Lippincott Company.
21. Erer KS. 2007 Adaptive usage of the Butterworth digital filter. *J. Biomech.* **40**, 2934–2943. (doi:10.1016/j.jbiomech.2007.02.019)
22. Sarrafian SK. 1983 *Anatomy of the foot and ankle: descriptive, topographic, functional*. Philadelphia, PA: JB Lippincott Company.
23. Myronenko A, Song X. 2010 Point set registration: coherent point drift. *IEEE Trans. Pattern Anal. Mach. Intell.* **32**, 2262–2275.
24. Marai GE, Laidlaw DH, Demiralp C, Andrews S, Grimm CM, Crisco JJ. 2004 Estimating joint contact areas and ligament lengths from bone kinematics and surfaces. *IEEE Trans. Biomed. Eng.* **51**, 790–799. (doi:10.1109/TBME.2004.826606)
25. Holowka NB, O'Neill MC, Thompson NE, Demes B. 2017 Chimpanzee and human midfoot motion during bipedal walking and the evolution of the longitudinal arch of the foot. *J. Hum. Evol.* **104**, 23–31. (doi:10.1016/j.jhevol.2016.12.002)
26. Welte L, Kelly LA, Lichtwark GA, Rainbow MJ. 2018 Influence of the windlass mechanism on arch-spring mechanics during dynamic foot arch deformation. *J. R. Soc. Interface* **15**, 20180270. (doi:10.1098/rsif.2018.0270)
27. Kessler SE, Lichtwark GA, Welte LKM, Rainbow MJ, Kelly LA. 2020 Regulation of foot and ankle quasi-stiffness during human hopping across a range of frequencies. *J. Biomech.* **108**, 109853. (doi:10.1016/j.jbiomech.2020.109853)
28. Farris DJ, Birch J, Kelly L. 2020 Foot stiffening during the push-off phase of human walking is linked to active muscle contraction, and not the windlass mechanism. *J. R. Soc. Interface* **17**, 20200208. (doi:10.1098/rsif.2020.0208)
29. Farris DJ, Kelly LA, Cresswell AG, Lichtwark GA. 2019 The functional importance of human foot muscles for bipedal locomotion. *Proc. Natl Acad. Sci. USA* **116**, 1645–1650. (doi:10.1073/pnas.1812820116)
30. de Ruiter CJ, van Oeveren B, Francke A, Zijlstra P, van Dieen JH. 2016 Running speed can be predicted from foot contact time during outdoor over ground running. *PLOS ONE* **11**, e0163023. (doi:10.1371/journal.pone.0163023)
31. Winter DA. 2009 *Biomechanics and motor control of human movement*, pp. 82–106. Hoboken, NJ: John Wiley & Sons, Inc.
32. Venkadesan M, Yawar A, Eng CM, Dias MA, Singh DK, Tommasini SM, Haims AH, Bandi MM, Mandre S. 2020 Stiffness of the human foot and evolution of the transverse arch. *Nature* **579**, 97–100. (doi:10.1038/s41586-020-2053-y)
33. Carlson RE, Fleming LL, Hutton WC. 2000 The biomechanical relationship between the tendoachilles, plantar fascia and metatarsophalangeal joint dorsiflexion angle. *Foot Ankle Int.* **21**, 18–25.
34. Cheng H-YK. 2008 Finite element analysis of plantar fascia under stretch—the relative contribution of windlass mechanism and Achilles tendon force. *J. Biomech.* **41**, 1937–1944.
35. Lovejoy CO, Latimer B, Suwa G, Asfaw B, White TD. 2009 Combining prehension and propulsion: the foot of *Ardipithecus ramidus*. *Science* **326**, 72–72e8. (doi:10.1126/science.1175832)
36. Sichting F, Holowka NB, Ebrecht F, Lieberman DE. 2020 Evolutionary anatomy of the plantar aponeurosis in primates, including humans. *J. Anat.* **237**, 85–104. (doi:10.1111/joa.13173)
37. Welte L, Kelly LA, Kessler SE, Lieberman DE, D'Andrea SE, Lichtwark GA, Rainbow MJ. 2020 Data from: The extensibility of the plantar fascia influences the windlass mechanism during human running. Dryad Digital Repository. (doi:10.5061/dryad.v9s4mw6sz)